Autocorrelation spectroscopy on single ultrathin layers of CdSe/ZnSe: hints for a non-thermal distribution of excitons in quantum islands

G. VON FREYMANN*, E. KURTZ*, C. KLINGSHIRN*, D. LITVINOV†, D. GERTHSEN†, T. H. SCHIMMEL* & M. WEGENER*

Institut für Angewandte Physik, Universität Karlsruhe (TH), 76128 Karlsruhe, Germany.
†*Laboratorium für Elektronenmikroskopie, Universität Karlsruhe (TH), 76128 Karlsruhe, Germany*

Summary

Autocorrelation spectroscopy on the basis of thousands of individual near-field photoluminescence spectra of single ultrathin CdSe layers at low temperatures exhibits a strong positive correlation peak around 18 meV energy with a width of 5 meV. Using simulations and experiments as a function of temperature and laser intensity, we can exclude interpretations along the lines of biexcitons or phonon sidebands. We attribute this feature to the splitting of ground state and an excited state in individual quantum islands. This interpretation implies that the potential minima are rather uniform in size and that the distribution of excitons is nonthermal.

Introduction

Epitaxially grown, thin semiconductor layers often lead to a series of sharp photoluminescence lines in near-field or microphotoluminescence experiments (Hess *et al.*, 1994; Zrenner *et al.*, 1994; Flack *et al.*, 1996; Jahn *et al.*, 1997; Robinson *et al.*, 1999; Wu *et al.*, 1999). These individual spectra can exhibit many tens or even hundreds of individual lines and usually look, at first sight, like a random distribution.

Autocorrelation spectroscopy allows us to extract more information by focusing on statistically significant features in all spectra: calculation of the autocorrelation for each spectrum and subsequent averaging over all autocorrelations allows for global statements about the potential landscape. Correlations in the spectrum can arise from correlations in the potential or from a potential which is just

Correspondence to: G. von Freymann. Tel: +49 721 608 3407; fax: +49 721 607 593; e-mail: georg.freymann@physik.uni-karlsruhe.de

noise. The first case would lead to positive correlations, the latter to negative correlations, i.e. to the so-called level repulsion (Runge & Zimmermann, 1998, 1999).

Recent experiments with ultrathin CdSe/ZnSe samples have shown a strong positive correlation feature around 18 meV energy with a width of 5 meV (von Freymann *et al.* 2000). In this article, we first briefly review the method called autocorrelation spectroscopy and then focus on the origin of the correlation feature.

Statistical analysis

Autocorrelation spectroscopy is based on the high lateral resolution achieved in microphotoluminescence or near-field optical experiments combined with the capability to measure huge sets of spectra from different locations on the sample within a reasonably short time. The huge amount of data is the precondition for the statistical analysis. In von Freymann *et al.* (2000) we have extended a proposal by Runge & Zimmermann (1998, 1999) and have made it suitable for experimental data.

Here we summarize this procedure: (1) normalization of the individual spectra to equal spectral integral; (2) subtraction of the average of these normalized spectra; $\delta I_n(\hbar\omega) = I_n(\hbar\omega) - \langle I_n(\hbar\omega)\rangle$; (3) calculation of the individual autocorrelations, $C(\Delta E) = \int \delta I_n(\hbar\omega') \, \delta I_n(\hbar\omega' + \Delta E) \, d\omega'$; (4) averaging over all individual autocorrelations; and (5) normalization of the maximum of $\langle C(\Delta E)\rangle$ at $\Delta E = 0$ to unity. For photoluminescence spectra $I(\hbar\omega)$, which consist of a series of sharp lines, i.e. $I(\hbar\omega) = \Sigma_n \, I_n\delta(\hbar\omega - (\hbar\omega_n))$ with arbitrary values of I_n, one can show that $\int_{-\infty}^{\infty} \langle C(\Delta E)\rangle d(\Delta E) = 0$ holds under these conditions.

We test this procedure with different sets of computer-generated random spectra. In these random spectra we have

chosen the number of lines, their width and their (Gaussian) distribution roughly to match both the individual measured spectra and their average. All data sets are treated with the same program. For the computer-generated spectra, we find a maximum at $\Delta E = 0$ and no further structure. The same behaviour is found in many other computer-generated sets with different numbers of lines and/or different distributions (not shown). This result is expected and illustrates that the defined procedure does not lead to artefacts.

Experiment and results

For the optical experiments we frequency-double about 1 W power at 800 nm wavelength from a continuous wave Ti:sapphire laser in a 2-mm thick BBO crystal to obtain about 3 μW power at 400 nm wavelength (3.10 eV photon energy). The excitation power can be continuously attenuated using a sequence of two polarizers. In the parallel polarized position, 200–300 nW are effectively coupled into an optical fibre. The light propagates towards a nanometer scale apex which is formed by a two-step selective etching process. Electron micrographs of identical fibre tips have been shown in Adelmann *et al.* (1999). The samples are mounted in a continuous-flow cryostat and can be temperature stabilized in a range from 4.2 to 310 K. The photoluminescence is collected with the same fibre and sent into a 0.5-m grating spectrometer (1800 lines/mm grating), which is connected to a liquid nitrogen cooled, back-illuminated, charge-coupled-device camera. The spectral resolution of this system is 0.06 nm, which is equivalent to an energy resolution of 250 μeV in the spectral range investigated. We scan the uncoated fibre tip at a constant height of 100 nm above the surface, i.e. the feedback loop is inactive. Under these conditions, the measured spatial resolution is better than $\lambda/5$ of the photoluminescence wavelength (540 nm). The data sets shown in the following are always based on 1600 individual spectra, each with 0.5 s exposure time of the charge-coupled-device camera, taken in a 2-μm × 2-μm area with 50 nm (100 nm) separation between adjacent points. For the intensity-dependent measurements, only 400 spectra from the same area are collected, with exposure times up to 10 s. We have carefully adjusted the exposure time for each measurement in order to maintain the same signal-to-noise ratio.

The four samples A, B, C and D are nominally ultrathin CdSe layers (2.0–3.6 monolayers) between ZnSe barriers. They are described in more detail in von Freymann *et al.* (2000) and the references therein. The individual photoluminescence spectra of these samples look very different in terms of line density and width of the line distribution. Also, they are shifted in the overall spectral position $\hbar\omega_0$ (left-hand side of Fig. 1). However, the correlation feature found by autocorrelation spectroscopy is very similar for many
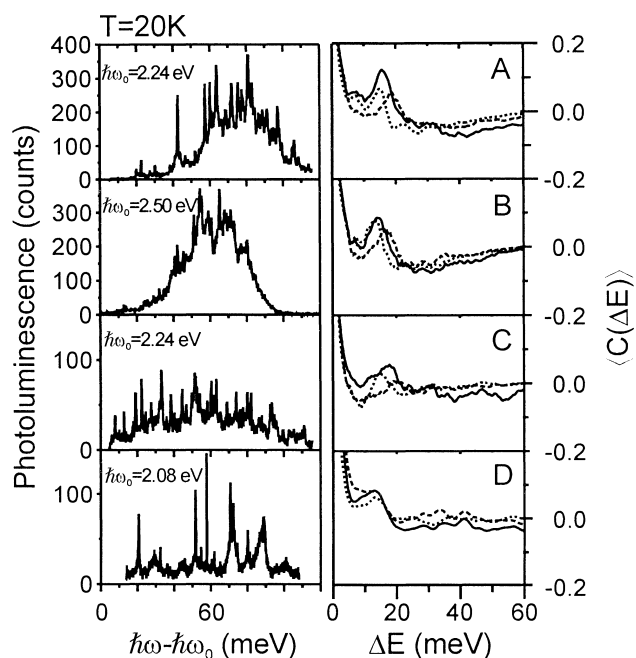
Fig. 1. One individual spectra of each sample A, B, C and D is shown on the left-hand side. The averaged autocorrelations for these data are displayed on the right-hand side: raw data (solid line), filtered data with $E_0 < 0$ (dashed line), filtered data with $E_0 > 0$ (dotted line). Filter function is $f(\hbar\omega) \propto \exp(\hbar\omega/E_0)$.

different measurements on samples A, B, C and D (right-hand side of Fig. 1). Therefore, the correlations in the photoluminescence lines of these CdSe/ZnSe layers seem to be generic for this material system.

Discussion

The correlations in the spectra can have different origins: Gindele *et al.* (1999) observed a broad (9 meV) phonon replica in these material systems as a result of the strong coupling of the exciton to the mixed state of ZnSe and CdSe LO-phonons. Also, they reported a strong biexcitonic emission 20 meV below the exciton peak. In addition, several researchers (Flack *et al.*, 1996; Peranio *et al.*, 2000) have reported islands in this material system with an areal density around 10^{11} cm^{-2} and with sizes of 5–10 nm (see Fig. 2b). Islands of rather uniform size ('self-organized quantum dots') would lead to a rather uniform level spacing (Fig. 2a). The internal motion of the electron and the hole within the exciton would lead to a further smearing-out, and hence to a broadening, of the potential for the excitons (Runge & Zimmermann (1999) (for bulk CdSe, the exciton Bohr radius is 9 nm). The expected level spacing for such effective potential wells is roughly consistent with the correlation energy of 18 meV observed in our work (the exciton mass of bulk CdSe is $1.3 \times m_0$, that of ZnSe
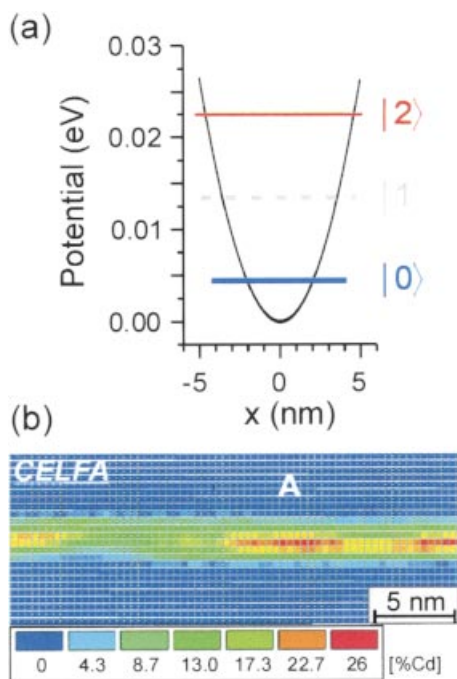
Fig. 2. (a) Simple model for a potential minimum in a quantum island of type A that results in a level spacing of about 18 meV. The ground state and the second excited state of the exciton are optically allowed. (b) The lateral dimensions are consistent with the sizes found for real islands in the sample by cross-section high-resolution transmission electron microscopy. The images are analysed by the composition evaluation by lattice fringe analysis (CELFA) routine described in detail by Rosenauer & Gerthsen (1999). The analysis yields the local Cd concentration that is displayed in a colour-coded map. Islands consisting of Cd-rich regions with sizes below 10 nm are clearly visible.

$1.9 \times m_0$) (see Fig. 2(a)). Also, the number of lines in each spectrum is roughly consistent with an areal density of islands of 10^{11} cm^{-2}.

The correlations are consistent with individual photoluminescence spectra, which consist of sets of pairs of lines. For each pair the energy spacing has to be around 18 meV. For an interpretation along the lines of a phonon sideband or of biexcitonic emission we would like to know whether the second peak lies on the low or on the high energy side of the first peak. To achieve this information, we multiply the individual photoluminescence spectra with filter functions $f(\hbar\omega)$ before performing step (1). Exponential functions, i.e. $f(\hbar\omega) \propto \exp(\hbar\omega/E_0)$, are especially simple to interpret. For the case of $E_0 < 0$ and for spectra that consist of pairs of lines with one main line and a weaker, low-energy sideband, the sideband would be enhanced by a certain factor (independent on its absolute energetic position). Consequently, the correlation function $\langle C(\Delta E)\rangle$ would exhibit enhanced correlations. Similarly, a high-energy sideband would be suppressed for $E_0 < 0$ and vice versa for $E_0 > 0$.

This idea has been verified explicitly by numerical simulation (not shown). Applying this procedure to the data leads to the curves shown in Fig. 1 on the right-hand side and in Fig. 3(b) (full lines correspond to the raw data, dotted lines to $E_0 = +18$ meV, dashed lines to $E_0 = -18$ meV). Obviously, the determined height of the correlation peak is roughly the same for $E_0 = \pm 18$ meV. This implies that we have pairs of lines with comparable strength – on average. This can either mean that the two lines in the pairs have identical strength in each case or that they fluctuate strongly independently. By additional simulations we have found that the latter scenario would lead to a correlation peak in $\langle C(\Delta E)\rangle$, which is definitely too weak to be consistent with the experiment (not shown). For lines of identical strength, our simulations (Fig. 3c) give results which are consistent with the experiment (Fig. 3b). Here we have chosen the parameters for the simulations such that the generated spectra match the experimental ones regarding line width, Gaussian distribution and spectral position (Fig. 3(a)).

Pairs of lines with comparable strength makes an interpretation along the lines of a phonon sideband unlikely (the LO-phonon energy of bulk CdSe is 26 meV, that of ZnSe is 32 meV. The observed correlation energy is below 20 meV for each sample). Furthermore, phonon sidebands in this
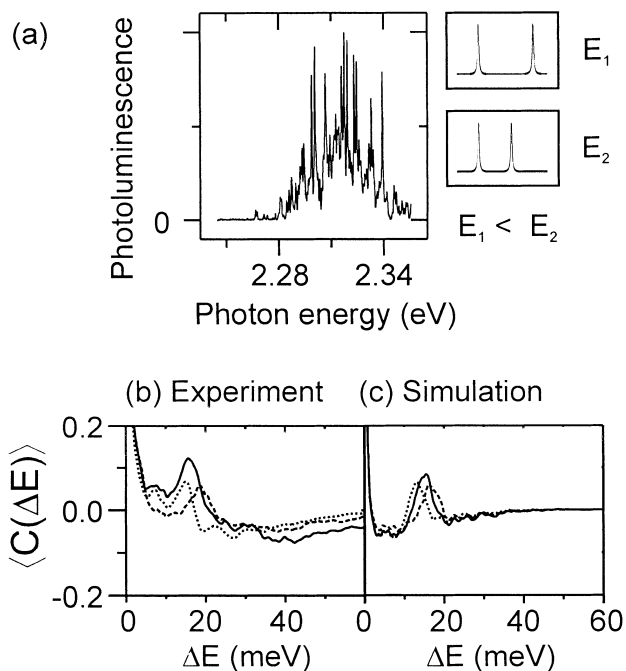
Fig. 3. (a) Individual simulated spectrum consisting of pairs of lines of equal strength. The energy spacing is chosen to match the experimental results. (b) Averaged autocorrelations for raw data (solid line), filtered data with $E_0 < 0$ (dashed line), filtered data with $E_0 > 0$ (dotted line). (c) same as (b) but for simulated data. Filter function is $f(\hbar\omega) \propto \exp(\hbar\omega/E_0)$.
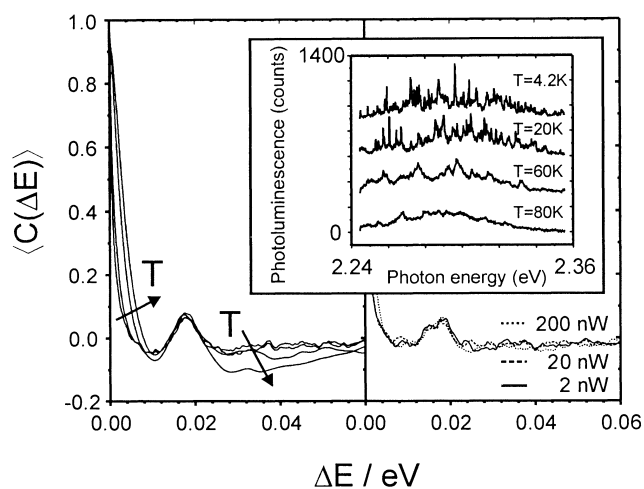
Fig. 4. Temperature dependence (left hand side) and intensity dependence at $T = 10$ K (right-hand side) of the correlation feature. The correlation feature remains unchanged even though the line width increases with increasing temperature and the sharp lines vanish (inset).

material system are not strong enough to explain the observed correlation feature ($I_{LO} = 0.04I_X$, Gindele *et al.*, 1999). Biexcitonic effects could also lead to pairs of lines of comparable strength. A clear signature of biexcitonic effects would be an intensity dependence. We have not found any intensity dependence when attenuating the incident laser intensity by two orders of magnitude, i.e. from 200 nW down to 2 nW excitation power (Fig. 4). However, it is interesting to note that the quantum dot biexciton binding energy of ≈ 20 meV observed in single-dot experiments (Bacher *et al.*, 1999; Gindele *et al.*, 1999) is close to the numbers seen here. We interpret the pairs of lines as ground and excited state of individual quantum islands. If this interpretation is correct, our observations would be evidence for a highly nonthermal distribution of excitons in these islands (resulting from the 'phonon bottle-neck'). In this case there should be no temperature dependence of the correlation feature; this is indeed the case. The correlation feature remains unchanged for temperatures in the range of $4.2 - 80.0$ K (Fig. 4). Note that the correlation feature is still present at high temperatures even though the sharp lines in the spectra have disappeared. All averaged autocorrelations are normalized to the value at $\Delta E = 0$. Looking at the raw autocorrelation data the total strength of the correlation feature decreases with decreasing photoluminescence intensity (for increasing temperatures). In addition to the energetic correlations, we also find spatial correlations in the photoluminescence maps. Numerical integration over each line in such a pair separately, shows a distribution rather lacking in order (Fig. 5). However, multiplication of the two photoluminescence maps with each other pointwise shows regions (marked by the dotted
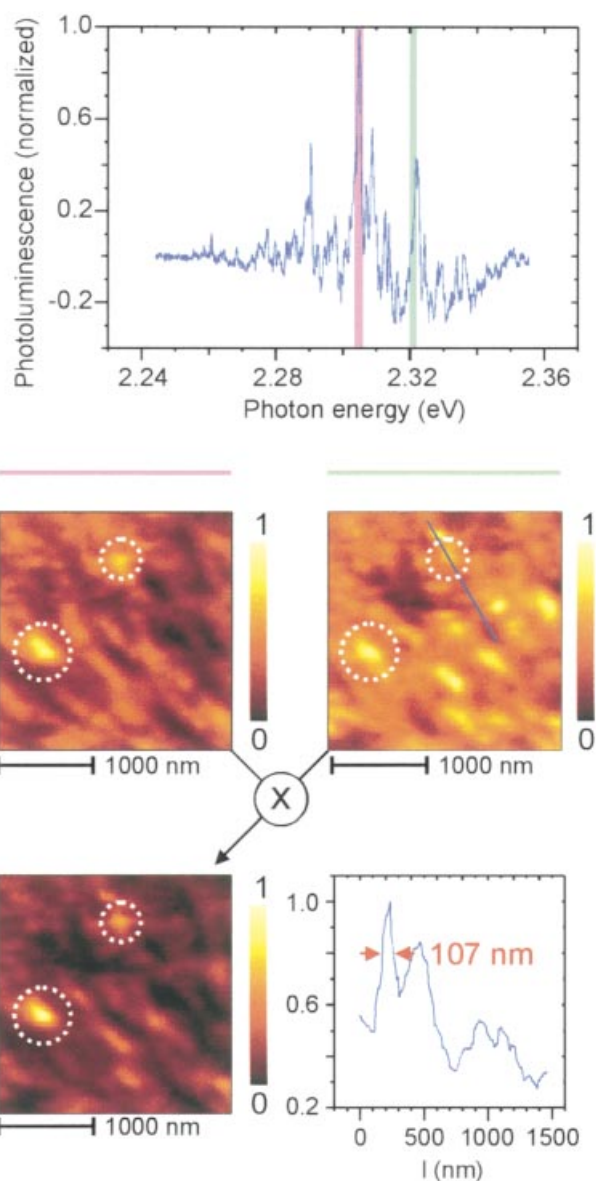
Fig. 5. One individual experimental spectrum after normalization and background subtraction. The photoluminescence maps of the red and the green highlighted areas are shown on the left, respectively, right-hand side. Pointwise multiplication of the photoluminescence maps clearly shows two areas where both lines can be found (dotted circles). The blue marked cross-section reveals a lateral resolution of 107 nm full width at half maximum, which is better than $\lambda/5$ of the photoluminescence wavelength.

circles in Fig. 5) where both lines are present. The lateral resolution, determined by a cross-section in one of the photoluminescence maps, is better than 110 nm (Fig. 5).

Conclusion

In conclusion, we have shown by simulations and direct experiments that the positive correlation feature found by

autocorrelation spectroscopy on ultrathin CdSe layers clad between ZnSe is not consistent with interpretations based on phonon sidebands or on biexcitonic emission. An interpretation along the lines of a nonthermal population of ground and an excited state in rather homogeneous quantum islands is consistent with the data.

Acknowledgements

References

Adelmann, Ch., Hetzler, J., Scheiber, G., Schimmel, Th., Wegener, M., Weber, H.B. & von Löhneysen, H. (1999) Experiments on the depolarization near-field scanning optical microscope. *Appl. Phys. Lett.* **74**, 179–181.

Bacher, G., Weigand, R., Seufert, J., Kulakovskii, V.D., Gippius, N.A. & Forchel, A. (1999) Biexciton versus exciton lifetime in a single semiconductor quantum dot. *Phys. Rev. Lett.* **83**, 4417–4420.

Flack, F., Samarth, N., Nikitin, V., Crowell, P.A., Shi, J., Levy, J. & Awschalom, D. (1996) Near-field optical spectroscopy of localized excitons in strained CdSe quantum dots. *Phys. Rev. B* **54**, R17312–R17315.

von Freymann, G., Kurtz, E., Klingshirn, C. & Wegener, M. (2000) Statistical analysis of near-field photoluminescence spectra of single ultrathin layers of CdSe/ZnSe. *Appl. Phys. Lett.* **77**, 394–396.

Gindele, F., Hild, K., Langbein, W. & Woggon, U. (1999) Phonon interaction of single excitons and biexcitons. *Phys. Rev. B* **60**, R2157–R2160.

Hess, H.F., Betzig, E., Harris, T.D., Pfeiffer, L.N. & West, K.W. (1994) Near-field spectroscopy of the quantum constituents of a luminescent system. *Science* **264**, 1740–1745.

Jahn, U., Ramsteiner, M., Hey, R., Grahn, H.T., Runge, E. & Zimmermann, R. (1997) Effective exciton mobility edge in narrow quantum wells. *Phys. Rev. B* **56**, R4387–R4390.

Peranio, N., Rosenauer, A., Gerthsen, D., Sorokin, S.V., Sedova, I.V. & Ivanov, S.V. (2000) Structural and chemical analysis of CdSe/ZnSe nanostructures by transmission electron microscopy. *Phys. Rev. B* **61**, 16015–16024.

Robinson, L.M., Rho, H., Kim, J.C. *et al.* (1999) Quantum dot exciton dynamics through a nanoaperture: evidence for two confined states. *Phys. Rev. Lett.* **83**, 2797–2800.

Rosenauer, A. & Gerthsen, D. (1999) Composition evaluation by the lattice fringe analysis method using defocus series. *Ultramicroscopy*, **76**, 49–60.

Runge, E. & Zimmermann, R. (1998) Spatially resolved spectra, effective mobility edge, and level repulsion in narrow quantum wells. *Phys. Stat. Sol. B* **206**, 167–174.

Runge, E. & Zimmermann, R. (1999) Level repulsion and wavefunction statistics in semiconductor quantum systems with localized excitons. *Ann. Phys.* **8**, 229–232.

Wu, Q., Grober, R.D., Gammon, D. & Katzer, D.S. (1999) Imaging spectroscopy of two-dimensional excitons in a narrow GaAs/AlGaAs quantum well. *Phys. Rev. Lett.* **83**, 2652–2655.

Zrenner, A., Butov, L.V., Hagn, M., Abstreiter, G., Böhm, G. & Weimann, G. (1994) Quantum dots formed by interface fluctuations in AlAs/GaAs coupled quantum well structures. *Phys. Rev. Lett.* **72**, 3382–3385.